Inorg. Chem. **2007**, *46*, 79–92

fac-{$Ru(CO)_3$}$^{2+}$-Core Complexes and Design of Metal-Based Drugs. Synthesis, Structure, and Reactivity of Ru–Thiazole Derivative with Serum Proteins and Absorption–Release Studies with Acryloyl and Silica Hydrogels as Carriers in Physiological Media

Renzo Cini,*,† Sandra Defazio,† Gabriella Tamasi,† Mario Casolaro,† Luigi Messori,‡ Angela Casini,‡ Margherita Morpurgo,§ and Michael Hursthouse||

Department of Chemical and Biosystem Sciences and Technologies, University of Siena, Via Aldo Moro 2, I-53100 Siena, Italy, Department of Chemistry, University of Florence, Via della Lastruccia 3, I-50019 Sesto Fiorentino, Italy, Department of Pharmaceutical Sciences, University of Padova, Via Marzolo 5, I-35131 Padova, Italy, and School of Chemistry, University of Southampton, Highfield, Southampton, SO17 1BJ, United Kingdom

Received May 4, 2006

The reaction of $[Ru_2(CO)_6Cl_4]$, **1**, with excess THZ (1,3-thiazole) in absolute ethanol at 55 °C produces *fac*-$[Ru(CO)_3Cl_2(THZ)]$, **2**, in high yield. $[Ru(CO)_2Cl_2(THZ)_2]$, **3**, is formed at higher temperature (ca 70 °C) and higher concentration of THZ. The X-ray structures of the new compounds have been determined, and density functional studies performed at the hybrid B3LYP/(Lanl2DZ, Ru; 6-311+G**, CHClNOS) level allowed the estimation of the structures of several conformers as well as that of their relative total electronic energies. Compound **2** is soluble (slowly) in aqueous media, where it reacts with the transport proteins bovine serum albumin (BSA) and human apotransferrin (HTF), and at a lower extent with calf thymus DNA (CT-DNA) and with guanosine-5′-monophosphate (GMP). The complex molecule is adsorbed by certain synthetic acryloyl polymers that have terminal carboxylate functions and is embedded in silica gels when these latter are prepared in the presence of a solution of **2**. Ruthenium species are slowly released from the loaded gels into physiological solutions at pH 7.4. The reactivity of **2** with biomolecules and synthetic hydrogels makes it a compound of interest for anticancer and antimetastases tests.

Introduction

The search for novel platinum group metal complexes that exhibit appreciable water solubility and the capacity to link to nucleobases, DNA fragments, aminoacids, peptides, and proteins is worthy of effort because of their potential as anticancer and antimetastases agents. Recently, the importance of *fac*-{$Tc/Re(CO)_3$}-core-containing complexes as possible radiodiagnostic and anticancer agents has been noted by Alberto and co-workers.[1]

On another side, the design of more efficient routes for administration of pharmaceutical compounds, especially metal-based drugs, is an important task to improve the efficacy of treatment and to lower the incidence of undesired side effects and toxicity to healthy tissues.

Ruthenium coordination compounds are currently the most promising metal-based chemotherapeutics after platinum compounds, and some of them are being intensively studied in clinical trials to fight metastases and colon cancer. Examples

* Author to whom correspondence should be addressed. Phone: +39.0577.234368. Fax: +39.0577.234177. E-mail: cini@unisi.it.
† University of Siena.
‡ University of Florence.
§ University of Padova.
|| University of Southampton.

(1) Zobi, F.; Spingler, B.; Fox, T.; Alberto, R. *Inorg. Chem.* **2003**, *42*, 2818.

(2) (a) Jakupec, M. A.; Reisner, E.; Eichinger, A.; Pongratz, M.; Arion, V. B.; Galanski, M.; Hartinger, C. G.; Keppler, B. K. *J. Med. Chem.* **2005**, *48*, 2831. (b) Kapitza, S.; Pongratz, M.; Jakupec, M. A.; Heffeter, P.; Berger, W.; Lackinger, L.; Keppler, B. K.; Marian, B. *J. Cancer Res. Clin. Oncol.* **2005**, *131*, 101. (c) Ni Dhubhghaill, O. M.; Hagen, W. R.; Keppler, B. K.; Lipponer, K.-G.; Sadler, P. J. *J. Chem. Soc. Dalton Trans.* **1994**, 3305. (d) Egger, A.; Arion, V. B.; Reisner, E.; Cebrián-Losantos, B.; Shova, S.; Trettenhahn, G.; Keppler, B. K. *Inorg. Chem.* **2005**, *44*, 122. (e) Reisner, E.; Arion, V. B.; Guedes, da Silva, M. F. C.; Lichtenecker, R.; Eichinger, A.; Keppler, B. K.; Yu, Kukushkin, V.; Pombeiro, A. J. L. *Inorg. Chem.* **2004**, *43*, 7083. (f) Arion, V. B.; Reisner, E.; Fremuth, M.; Jakupec, M. A.; Keppler, B. K.; Yu, Kukushkin, V.; Pombeiro, A. J. L. *Inorg. Chem.* **2003**, *42*, 6024. (g) Piccioli, F.; Sabatini, S.; Messori, L.; Orioli, P.; Hartinger, C. G.; Keppler, B. K. *J. Inorg. Biochem.* **2004**, *98*, 1135.

10.1021/ic060755s CCC: $37.00
Published on Web 12/10/2006

are *trans*-[$RuCl_4(IM)_2$](IMH) (IM = 1,3-imidazole) (ICR) and *trans*-[$RuCl_4(ID)_2$](IDH) (ID = indazole) (KP1019, FFC14A) and related complexes by Keppler and co-workers[2] and *trans*-[$RuCl_4$(IM)(*S*-DMSO)](IMH) (DMSO = dimethyl sulfoxide), NAMI-A, by Alessio and Sava and their co-workers.[3] These ruthenium complexes are considered as prodrugs because the activity seems to be initiated by a reduction from Ru(III) to Ru(II) once the core complex is inside the anoxic cancer tissues, followed by linkage to nucleic acids. Notwithstanding, it has to be noted that very little is known about the ultimate mechanism for anticancer and antimetastases activity, as compounds that are not appreciably cytotoxic like NAMI-A appear to be the most promising ruthenium-based compounds for the treatment of human cancer to date. Therefore, the primary task for researchers in the field of biocoordination chemistry is to look for compounds that have an appreciable solubility in physiological media and have the capability to link somewhat to transport and store biomolecules. Whenever a compound that possesses these properties is selected and characterized, subsequent tests devoted to determining biological activity in vivo as anticancer, antimetastases, anti-inflammatory agents and to measuring the toxic effects on healthy tissues should be carried out, regardless of whether the cytotoxic activity in vitro is significant or not.

We reasoned that Ru(II) complexes that have both appreciable solubility in aqueous media and uptake by the cell are likely to produce more active compounds because the reduction step is skipped. Furthermore, we looked for materials that can deliver the compound to the target tissues via a multistep procedure that consists of (a) embedding of the drug, (b) implantation of the loaded material into the body close to the diseased tissue, and (c) a slow and constant release of the metal-based drug in such a way as to reach the high concentration specifically in the target tissue.

On the basis of this reasoning, we first looked for low molecular weight Ru(II) complexes with a suitable solubility in water. Then we searched for synthetic polymers that could be tolerated by living tissues, that are able to adsorb relatively large amounts of the metal compound, and finally that are able to release the compound under controlled conditions in such a way as to give concentrations suitable for reaching an acceptable pharmaceutical activity with no appreciable toxicity for the healthy tissue.

Our attention was first focused on the *fac*-$\{Ru(CO)_3\}^{2+}$-core-containing complexes, because the $Ru(CO)_3$ core is chemically inert (the presence of the carbonyl stabilizes the low oxidation state) and the extra ligands can be released at an acceptable rate because the significant trans effects from the three COs.

The chemistry of halogen−carbonyl−ruthenium compounds was first studied and reported by several workers many years ago[4] and more recently by others.[5] We found that *fac*-[$Ru(CO)_3Cl_2$(THZ)] (THZ = 1,3-thiazole) can be prepared in high yield via an efficient one-step synthesis from commercial $[Ru(CO)_3Cl_2]_2$. Through the same synthesis *cis*,*trans*,*cis*-[$Ru(CO)_2(Cl_2)(THZ)_2$] can be obtained. Here we wish to report on the synthesis, the structural characterization, the solution behavior of the two derivatives, as well as the preliminary reactivity of the monothiazole derivative with selected biomolecules and synthetic polymers.

Experimental Section

Materials. $[Ru_2(CO)_6Cl_4]$ (**1**) was purchased from Strem Chemicals (Newburyport, MA) and used without any further purification. The purity was checked via IR spectroscopy.

The IR spectrum from spectroscopy-grade chloroform has only two peaks in the region of the carbonyl vibrations: a sharp and strong band at 2137 cm^{-1} and a strong band at 2069 cm^{-1} with a shoulder at 2064 cm^{-1}. On the basis of the assignment reported in ref 4, the product is considered consistent with the presence of only one species that is identified as *fac*-$[Ru(CO)_3Cl_2]_2$. Thiazole (THZ, reagent grade) was from Alfa Aesar a Johnson Matthey company (Ward Hill, MA). Tris(hydroxymethyl)aminomethane (TRIS) and tris(hydroxymethyl)aminomethane hydrochloride ($HTRIS^+Cl^-$) were biochemical grade, purchased from Acros Organics (Geel, Belgium) and used without further purification. $NaH_2PO_4 \cdot H_2O$ was an analytical grade product from J.T. Baker (Deventer, Holland). Tetraethoxysilane (TEOS) was obtained from Sigma (St. Louis, MO). HCl, NaOH, NaCl, Na_2CO_3, $NaHCO_3$, molibdic acid, ascorbic acid, benzoic acid (HBA), and all the solvents were analytical grade from Sigma. $Na_2GMP \cdot 4H_2O$ (guanosine-5′-monophosphate disodium salt tetrahydrate), iron-free human transferrin (siderophilin, human apotransferrin, HTF), and deoxyribonucleic acid (DNA) from calf thymus (type I, 5.1% Na, 8.5% H_2O) and bovine serum albumin (BSA) were purchased from Sigma-Aldrich (Milan, Italy). L-phenylalanine, acryloyl chloride, *N*,*N*′-ethylenebisacrylamide (EBA) were purchased from Fluka Co. *N*-Isopropylacrylamide (NIPAAM) was from Sigma-Aldrich (Milan, Italy). Amicon ultracentrifugal filters, 30 kDa, were purchased from Millipore (Bedford, MA).

Synthesis. *fac*-[$Ru(CO)_3Cl_2$(THZ)] (2). Two-hundred milligrams of **1** (0.39 mmol) was ground to a fine powder in an agate mortar and then mixed with absolute ethanol (8 mL). The mixture was stirred in the air atmosphere at 25 °C up to complete dissolution of the white powder (in the case where the dissolution is slow, a gentle heating up to 40 °C was applied). Excess thiazole (150 mg, 1.76 mmol) was added to the clear solution of **1** and the final mixture was stirred at 55 °C for 2 h in the dark. The pale yellow solution was allowed to slowly cool down to 25 °C and then stored for 24 h in the dark. On cooling and concentrating to ca. half volume (through spontaneous evaporation of solvent), the solution produced long, colorless, parallelepiped-shaped crystals. The crystals were filtered off, rinsed three times with small portions of cool absolute ethanol, and then dried in the air atmosphere for 12 h. It has to be pointed out that in the case where the mother solution is refluxed (78 °C) or is concentrated to a very small volume, a mixture of products precipitates (see below). Yield: 50%. IR: KBr matrix,

(3) (a) Velders, A. H.; Bergamo, A.; Alessio, E.; Zangrando, E.; Haasnoot, J. G.; Casarsa, C.; Cocchietto, M.; Zorzet, S.; Sava, G. *J. Med. Chem.* **2004**, *47*, 1110. (b) Bacac, M.; Hotze, A. C. G.; van der Schilden, K.; Haasnoot, J. G.; Pacor, S.; Alessio, E.; Sava, G.; Reedijk, J. *J. Inorg. Biochem.* **2004**, *98*, 402. (c) Sava, G.; Capuzzi, I.; Clerici, K.; Gagliardi, R.; Alessio, E.; Mestroni, G. *Clin. Exp. Metastasis* **1998**, 371.

(4) Johnson, B. F. G.; Johnston, R. D.; Lewis, J. *J. Chem. Soc. (A)* **1969**, 792.

(5) (a) Alessio, E. *Chem. Rev.* **2004**, *104*, 4203. (b) Alessio, E.; Milani, B.; Bolle, M.; Mestroni, G.; Faleschini, P.; Todone, F.; Geremia, S.; Calligaris, M. *Inorg. Chem.* **1995**, *34*, 4722.

2135 cm^{-1} (sharp, sh; strong, s), 2044 cm^{-1} (br, br; s); CH_2Cl_2 solution (0.17 mol L^{-1}), 2135 cm^{-1} (sh, s), 2073 cm^{-1} (sh), 2048 cm^{-1} (sh, s). UV: MeOH (anhydrous, 25 °C), 230 nm (ϵ, 8500 cm^{-1} mol^{-1} L), shoulder 276 nm (2000); DMSO, shoulder 289 nm (1970). Anal. Calcd for $C_6H_3Cl_2NO_2RuS$ (M_w, 341.13): C, 21.21; H, 0.89; Cl, 20.78; N, 4.11; S, 9.40. Found: C, 21.12; H, 1.01; Cl, 20.7; N, 4.14; S, 9.37. On heating, crystals of **2** change their shape starting at 170 °C when observed through polarized light under a Kofler-type microscope; complete melting was reached at 180 ± 3°C. Evolution of gas happens before melting. The color under white light does not change up to 185 °C.

***cis,trans,cis*-[Ru(CO)$_2$Cl$_2$(THZ)$_2$] (3). Procedure A.** The mother solution from the preparation of **2** was heated up to reflux for two more hours. The final yellow solution was left to cool down to 25 °C and to concentrate by slow evaporation of the solvent in the air. Yellow crystals formed after 24 h. They were collected by filtration, washed with cool ethanol, and then dried in the air for 24 h. Yield: 35%. Analytical and spectroscopic data were as for the product from procedure B (see below), within experimental errors.

Procedure B. Two-hundred milligrams of **1** (0.39 mmol) was mixed with absolute ethanol (8 mL) after grinding to a fine white powder. The mixture was stirred in the air atmosphere at 25 °C up to complete dissolution of the white powder (in the case where the dissolution is slow, a gentle heating up to 40 °C was applied). Excess thiazole (150 mg, 1.76 mmol) was added to the clear solution of **1** and the final mixture was stirred under reflux for 2 h in the dark. The final yellow solution was concentrated to ca. 2 mL via evaporation of the solvent and then stored. After ca. 24 h yellow crystals formed. They were collected by filtration, washed with cool ethanol, and then dried in the air for 24 h. Yield: 70%. IR: KBr matrix, 2055 cm^{-1} (sh, s), 1984 cm^{-1} (br, s), shoulder 1943 cm^{-1} (medium, m). UV: MeOH (anhydrous, 25 °C), 235 nm (10 900), 370 nm (441). Anal. Calcd for $C_8H_6Cl_2N_2O_2RuS_2$ (M_w, 389.30): C, 24.13; H, 1.52; Cl, 17.7; N, 7.03. Found: C, 24.23; H, 1.45; Cl, 17.2; N, 7.19.

***fac*-[Ru(CO)$_3$(OH)(THZ)(OOCC$_6$H$_5$)]·H$_2$O (4)**. An aqueous suspension of benzoic acid (HBA) (0.20 mmol in 4 mL) was heated up to 80 °C and gently stirred up to complete dissolution of the crystalline solid. At that point the solution was cooled down to 25 °C and brought up to pH 5.5 by dropwise addition of NaOH(aq). This solution was added to an aqueous solution of **2** (0.10 mmol in 4 mL), under stirring for 2 h at 25 °C. The solutions of **2** and HBA/BA were then mixed and the mixture was maintained at 40 °C under stirring for 3 h. A red precipitate formed. The suspension was concentrated to a quarter of the initial volume by evaporation under a stream of nitrogen and then filtered. The red solid was filtered off, rinsed with 1 mL of cold water (three times), and then dried in the air. Yield: 35%. IR: KBr matrix, 2056 cm^{-1} (s), 1975 (s), 1938 (s). Anal. Calcd for $C_{13}H_{11}NO_7RuS$ (M_w, 426.38). C, 36.61; H, 2.60. Found. C, 35.95; H, 2.46.

***N*-Acryloyl-L-phenylalanine (5).** The vinyl monomer **5** (HPHE) was synthesized according to a previously reported procedure.[6] Briefly, to a well-stirred aqueous solution (100 mL) of L-phenylalanine (0.33 mol) and sodium hydroxide (0.67 mol) was added acryloyl chloride (0.31 mol) dropwise over a 30 min period. The reaction mixture was kept at a temperature below 0 °C by cooling with an external ice bath. Then, the mixture was acidified to pH 2 with HCl (37%, 28 mL). The voluminous white product was filtered off and the monomer was recovered by crystallization from hot water. Elemental, spectroscopic (^{1}H NMR, IR), and potentiometric analyses were consistent with an analytical grade product.

***fac*-[Ru(CO)$_3$(OH)(THZ){OOCCH(CH$_2$C$_6$H$_5$)NHCOCH=CH$_2$}]·H$_2$O (6).** Sixty-four milligrams of HOOCCH(CH$_2$C$_6$H$_5$)-NHCOCH=CH$_2$ (HPHE, 0.29 mmol) was dissolved in water (9 mL) at 25 °C with stirring. Heating the suspension to increase the solution rate has to be avoided to decrease the formation of polymeric species. The pH of the solution was adjusted to 6 by adding dilute NaOH(aq). Forty-seven milligrams of a fine powder of **2** (0.14 mmol) was dissolved in water (4 mL), with stirring for 2 h at 25 °C. The solutions of **2** and HPHE were then mixed and the mixture was maintained at 25 °C with stirring for 12 h. The beige precipitate that formed was filtered off, rinsed three times with 2 mL of cool water, and then dried in the air for 24 h. Yield: 35%. IR: KBr matrix, 2033 cm^{-1} (s), 1949 (s). ^{1}H NMR: compound **6** is appreciably soluble in DMSO-d_6 only, and the ^{1}H NMR spectrum in that solvent is practically superimposable with that for free HPHE in the relevant spectrum region; this suggests that the ligand is removed by solvent molecules shortly after dissolution. Anal. Calcd for *fac*-[Ru(CO)$_3$(OH)(THZ)(PHE)]·H$_2$O, $C_{18}H_{18}N_2O_8SRu$ (M_w, 523.47): C, 41.30; H, 3.47; N, 5.35; S, 6.13. Found: C, 41.16; H, 3.50; N, 4.71; S, 6.42.

***fac*-[Ru(CO)$_3$(THZ)(GMP)]·6H$_2$O (7).** Forty-eight milligrams of Na$_2$GMP·4H$_2$O (0.10 mmol) was dissolved in water (2.5 mL). The solution of the nucleotide was added to an aqueous solution of **2** (0.10 mmol; 15 mL) and the final mixture was stirred in the dark at 25 °C overnight. The solution was concentrated to a final volume of 4 mL by evaporation under a stream of dry nitrogen; an orange precipitate formed: it was collected via filtration, washed twice with 1 mL of water at 5 °C, and then dried in air. Yield: 30%. IR: KBr matrix, 2039 cm^{-1} (s), 1990 (s), 1986 (s). Anal. Calcd for $C_{16}H_{27}N_6O_{17}PRuS$ (M_w, 739.53): C, 25.99; H, 3.68; N, 11.36; P, 4.19; S, 4.34. Found: C, 25.35; H, 3.22; N, 11.0; P, 4.10; S, 4.06.

Acryloyl Polymer (8). The synthesis of the poly(*N*-acryloyl-L-phenylalanine-*co*-*N*-isopropylacrylamide) in the free and in the cross-linked form was previously reported.[6] Two water-soluble (*co*-0.1 and *co*-10) and one swellable hydrogel (CP2) were chosen for the present investigation. The copolymers *co*-0.1 and *co*-10 were made of the two monomers, purchased NIPAAM and prepared PHE, containing 10 and 83 wt % of PHE units, respectively; CP2 was a copolymer with a NIPAAM/PHE molar ratio of 10 and cross-linked with 2 mol % EBA. Elemental and IR analyses were consistent with an acceptable purity.

Silica Gels (9). Gels were synthesized from tetraethoxysilane by a two-step acid−base catalyzed method according to a procedure described elsewhere.[7a] In short, acid-catalyzed hydrolysis of the alkoxysilane was carried out by 2 h reflux in absolute ethanol with catalytic amounts of water and HCl (Si:HCl:H$_2$O = 1:0.01:2). Gels (1.5 mL) were then obtained at room temperature by adding 0.818 mL of a ruthenium complex solution (12.4 mg mL^{-1} in ethanol/methanol, 90/10) to 0.609 mL of the prehydrolyzed solution, followed by 0.073 mL of Na_2CO_3, 0.22 mol L^{-1} in H$_2$O as a catalyst.[7b] Ruthenium-free matrices were obtained by the same protocol using ruthenium-free methanol:ethanol solution. Gelation occurred within 8 h. The gel was aged for 2 days in a closed vial and then the liquid, expelled as a consequence of the syneresis process, was removed. Gels were dried at 50 °C until constant

(6) Casolaro, M.; Paccagnini, E.; Mendichi, R.; Ito, Y. *Macromolecules* **2005**, *38*, 2460.

(7) (a) Morpurgo, M.; Teoli, D.; Palazzo, B.; Bergamin, E.; Realdon, N.; Guglielmini, M. *Farmaco* **2005**, *60*, 675. (b) Morpurgo, M.; Teoli, D.; Palazzo, B.; Realdon, N.; Guglielmini, M. European Conference on Drug Delivery and Pharmaceutical Technology, Sevilla, Spain, 2004.

Table 1. Crystal Data and Structure Refinement for *fac*-[$Ru(CO)_3Cl_2(THZ)$] **2** and *cis*,*trans*,*cis*-[$Ru(CO)_2Cl_2(THZ)_2$] **3** (radiation, λ(Mo Kα) = 0.710 73 Å)

	2, 293 K	**3**, 293 K	**3**, 120 K
empirical formula	$C_6H_3Cl_2NO_3RuS$	$C_8H_6Cl_2N_2O_2RuS_2$	$C_8H_6Cl_2N_2O_2RuS_2$
formula weight	341.12	398.24	398.24
crystal system, space group	monoclinic, *P*21/*c*	monoclinic, *C*2/*c*	monoclinic, *C*2/*c*
unit cell dimensions			
a (Å)	10.389(2)	7.256(1)	7.188(1)
b (Å)	18.465(3)	14.497(2)	14.348(3)
c (Å)	12.439(2)	13.004(1)	12.760(3)
β (deg)	111.02(2)	92.85(1)	93.21(3)
volume (Å^3)	2227.4(7)	1366.2(3)	1313.9(5)
Z, calcd density (Mg m^{-3})	8, 2.034	4, 1.936	4, 2.013
absorption coefficient (mm^{-1})	2.053	1.833	1.906
reflections collected/unique	4936/3927	1319/1218	6397/1498
R(int)	0.0264	0.0094	0.0212
data/restraints/parameters	3927/0/254	1218/8/98	1498/11/121
final *R* indices [$I > 2\sigma(I)$]	R1 = 0.0458	R1 = 0.0275	R1 = 0.0223
	wR2 = 0.1187	wR2 = 0.0613	wR2 = 0.0519
R indices (all data)	R1 = 0.0575	R1 = 0.0366	R1 = 0.0232
	wR2 = 0.1267	wR2 = 0.0660	wR2 = 0.0524
largest diff peak and hole (e Å^{-3})	1.043 and −0.890	0.345 and −0.335	0.538 and −0.735

weight; they were then ground and sieved to obtain granules with a homogeneous distribution of sizes (diameter, 63−200 μm).

Spectroscopy. IR. The infrared spectra of the solid samples were recorded via the KBr pellet technique or via the Nujol mull method. The spectra from aqueous solutions were recorded by using CaF_2 windows spaced by a layer of lead (0.1 mm thickness). The spectra from CH_2Cl_2, methanol, ethanol were recorded by using KBr or CsI windows (same spacer as above). All the spectra were obtained through a Perkin-Elmer Model 1600 FT-IR spectrometer.

UV−Vis. All the spectra were recorded by using 1-cm-depth quartz cuvettes and a Perkin-Elmer Model EZ 201 spectrophotometer.

CD. Circular dichroism spectra were obtained through a Jasco J-600 spectropolarimeter.

AAS, ICP-OES. Atomic absorption spectroscopy and inductively coupled plasma optical emission spectroscopy analyses of Ru were performed by using a Perkin-Elmer 5000 spectrometer operating with acetylene/air flame activation, a Perkin-Elmer Analyst100 spectrometer (continuum background correction) with electrothermal atomization in a graphite furnace, and a Perkin-Elmer Optima 2000 spectrometer. The stock solution of ruthenium was obtained by dissolving crystalline [$Ru(CO)_3Cl_2(THZ)$] (50 mg) in an aqueous solution of ultrapure hydrochloric acid (0.1 mol L^{-1}, 10 mL). The standard solutions were prepared immediately before the analysis by properly diluting the stock solution.

NMR. The spectra were recorded by using deuterated solvents at 99.8 atom D %, 0.01 mol L^{-1} concentrations of the compounds, and Varian XL-200 or Bruker DRX-600 spectrometers located at CIRM (Centro Interdipartimentale per le Risonanze Magnetiche, University of Siena).

Conductivity. The measurements of conductivity in methanol and methanol/water solutions were performed by using a Crison GLP32 conductivity-meter at 25 °C.

Ultrafiltration. An ALC PK110 centrifuge was loaded with Amicon Centricon YM-10 and YM-30 ultrafilters with threshold molecular weight of 10 and 30 kDa, respectively, that contain 4 mL of solution. The speed was maintained at 4000 rpm for 15 min. The UV absorption spectra of the upper and lower portions were recorded and AAS or ICP-OES measurements were performed as well on both the fractions.

Potentiometric Titrations. Potentiometric titrations were carried out in aqueous solutions (NaCl, 0.15 mol L^{-1}) at 25 °C, according to a previously described procedure.[8a] The measurements were done using a TitraLab 90 titration system from Radiometer Analytical. The titrations of the compounds were performed in a thermostated glass cell filled with 100 mL of NaCl (0.15 mol L^{-1}). An accurately weighed amount of the solid material and a measured amount of standard HCl (0.1 mol L^{-1}) were dispersed by stirring under a nitrogen stream. The titrant was standard NaOH (0.1 mol L^{-1}) solution. The equilibration time was 900 s for each titration step (0.04 mL).

X-ray Crystallography. *fac*-[$Ru(CO)_3Cl_2(THZ)$] (2). A well-formed colorless parallelepiped of dimensions 0.60 × 0.20 × 0.20 mm was selected under the polarizing microscope and then mounted on a glass capillary. Accurate cell dimensions (Table 1) were obtained by applying the least-squares technique to the values of 43 high angle, randomly selected, relatively strong reflections. The Siemens P4 four-circle automatic diffractometer at CIADS (Centro Interdipartimentale di Analisi e Determinazioni Strutturali, University of Siena) was used for the XRD measurements. A total of 4936 reflections were collected at 293 K, 3927 of which were unique and 3202 considered observed ($I > 2\sigma(I)$). The data set was corrected for Lorentz−polarization effects. The absorption correction was applied to the data set by using the ψ-scan method based on the values of nine reflections and the XEMP computer program.[9a]

The structure solution and refinement were performed via the direct methods and a series of twelve difference Fourier and least-squares cycles that located all the non-hydrogen atoms. Two complex molecules are present in the asymmetric unit. They differ by the orientation of the thiazole plane with respect to the equatorial plane defined by the two chloride ligands and two carbonyl ligands.

The hydrogen atoms were set in calculated positions via the HFIX/AFIX options of SHELX97[9b] implemented in WinGX[10] and they were left to ride on the atoms to which they are linked in the

(8) Casolaro, M.; Bottari, S.; Cappelli, A.; Mendichi, R.; Ito, Y. *Biomacromolecules* **2004**, *5*, 1325.

(9) (a) *XEMP, Empirical Absorption Correction*, Version 4.2 for MSDOS; Siemens Analytical X-Ray Inst. Inc., 1990. (b) Sheldrick, G.M. *SHELXS/L97 Programs for the Solution/Refinement of Crystal Structures*, University of Göttingen, Göttingen, Germany, 1997.

(10) (a) Farrugia, L. J. *WinGX an Integrated System of Windows Programs for the Solution, Refinement and Analysis of Single Crystal X-Ray Diffraction Data*, Version 1.64.05; University of Glasgow, Glasgow, UK, 1999−2003. (b) Farrugia, L. J. *J. Appl. Crystallogr.* **1999**, *32*, 837.

subsequent refinement cycles. All the non-hydrogen atoms were refined with anisotropic thermal parameters, whereas the hydrogen atoms were considered isotropically. The final conventional agreement factors were R1 0.0458 and wR2 0.1187 for the observed reflections.

The analysis of the molecular structure and molecular graphic computations were performed via PARST97[11] and ORTEP3.[12] All the computer programs were implemented under the WinGX package with Microsoft Windows-XP operating system.

***cis,trans,cis*-[$Ru(CO)_2Cl_2(THZ)_2$] (3). Data Set Collected at 293 K.** A well-formed yellow crystal of dimensions 0.60 × 0.35 × 0.35 mm was first mounted on a glass capillary and then submitted to X-ray diffraction experiments at 293 K through a Siemens P4 four-circle automatic diffractometer. The cell constant determination was based on the angles of 35 randomly selected high-angle and high-intensity reflections, by using the least-squares methods. The cell constants and other crystallographic parameters are reported in Table 1. The full data set consisted of 1319 reflections, 1218 of which were unique. The data set was corrected for Lorentz−polarization effects and then for the absorption effects via the ψ-scan technique. The number of observed reflections was 1062. The structure solution was performed via the direct methods of SHELX97[9b] and subsequent cycles of difference Fourier and least-squares computations. The thiazole molecules were affected by a statistical disorder simulated by noncrystallographic pseudo-C_2 axes passing on the Ru and the N(THZ) atoms. The disorder was solved by routine procedures that located C4 and S3 atoms for the two orientations. The disorder of C2 and C5 was not solved and only a position for each atom was refined. The hydrogen atoms on C2 and C5 were set in calculated positions and allowed to ride on the atoms to which they were linked during the subsequent refinement cycles. The H4 atom was not included at all in the refinement, because of its disorder. The conventional R1 and wR2 agreement factors converged to 0.0275 and 0.0613, respectively.

The analysis of the molecular structure revealed that the C−O carbonyl bond distances were unacceptably short, 1.053(5) Å. This anomaly was attributed to some type of disorder at the CO site whose analysis was not possible after many attempts. Therefore, it was decided to perform a further data collection at 120 K.

***cis,trans,cis*-[$Ru(CO)_2Cl_2(THZ)_2$] (3). Data Set Collected at 120 K.** A well-formed yellow crystal of dimensions 0.60 × 0.35 × 0.35 mm was mounted on a glass fiber and then submitted to X-ray diffraction experiments at 120 K through a Nonius Kappa CCD area detector situated at the window of a rotating anode (EPSRC, National Crystallographic Service, School of Chemistry, University of Southampton, Southampton, UK). The low-temperature device was an Oxford Instrument Cryo-stream.[13] Data were collected to a maximum 2θ value of 52°. Data processing was carried out through the COLLECT[14a] and DENZO[14b] software packages. Absorption corrections were applied using SADABS.[14c]

The structure solution and refinement was carried out via SHELX97[9b] by using the same strategies as those used for the data set collected at 293 K. Even the disorder of the thiazole molecule was treated in the same way. The difference Fourier map computed after all the atoms were located showed a significant residual electron density in the proximity of the carbonyl ligand and the chloride ligand. This was interpreted as an occupational disorder of carbonyl and chloride at the same coordination site. As a consequence, the occupancies (SOF) of the carbonyl, and the chlorine atoms were refined to sum up to 1. The SOFs refined to 0.88 for CO and 0.12 for Cl, whereas the thermal parameters converged to reasonable values for those atoms. This model was refined to final conventional agreement factors of R1 0.0223 and wR2 0.0519. All the hydrogen atoms were refined as isotropic, whereas all the heavy atoms were treated anisotropically. The Ru−Cl and Ru−CO bond distances converged to 2.375(1) and 2.337(9) Å, and 1.878(8) and 1.889(10) Å, which are very reasonable values, even though the structure is disordered.

Scheme 1. Drawing of the Possible More Stable Rotamers for *fac*-[$Ru(CO)_3Cl_2(THZ)$] as Viewed down the OC−Ru−N(THZ) Axis[a]

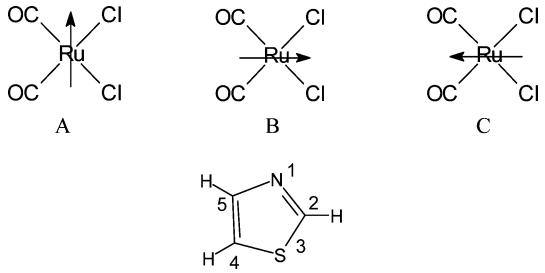

[a] The arrow represents the plane of the THZ ligand and is oriented along the C2−H vector. The apical carbonyl ligand is not represented for clarity purposes. The structural formula of 1,3-thiazole (THZ) with the numbering used in the text is also represented. Type-A and type-B rotamers only were found at the solid state. The rotation of THZ around the Ru−N bond is free in solution at room temperature.

Computational Methods. Ab Initio and Density Functional. All the computations were performed by using the Gaussian 98 package[15] implemented on IBM-SP4 and -SP5 clusters of computers at CINECA (Inter-University Consortium for Scientific Computation, Casalecchio di Reno, Bologna, Italy). The molecules investigated were *fac*-[$Ru(CO)_3Cl_2(THZ)$]-A, *fac*-[$Ru(CO)_3Cl_2(THZ)$]-B, and *fac*-[$Ru(CO)_3Cl_2(THZ)$]-C (Scheme 1), and *cis,trans,cis*-[$Ru(CO)_2Cl_2(THZ)_2$]-E and *cis,cis,trans*-[$Ru(CO)_2Cl_2(THZ)_2$]-F (Scheme 2). Some model molecules with NH_3 in the place of THZ ligands were also analyzed at different levels of basis sets. The level of theory used to compute the structures of the complexes [$Ru(CO)_3Cl_2(THZ)$] and [$Ru(CO)_2Cl_2(THZ)_2$] was B3LYP/(Lanl2DZ, Ru; 6-311++G**, CHNOSCl),[16] and the structure optimization was continued up to the threshold values implemented in Gaussian 98:[15] (maximum force 0.000 450 mdyn, root-mean-square (rms) force 0.000 300 mdyn, maximum displacement 0.001 800 Å, rms

(11) Nardelli, M. *PARST97, A System of Computer Routines for Calculating Molecular Parameters from Results of Crystal Structure Analyses;* University of Parma, 1997.
(12) Johnson, C. K.; Burnett, M. N. *ORTEP3 for Windows*; Oak Ridge National Laboratory, 1998; 32-bit Implementation by Farrugia, L. J. University of Glasgow, Glasgow, UK, 1999.
(13) Cosier, J.; Glazer, A. M. *J. Appl. Crystallogr.* **1986**, *19*, 105.
(14) (a) Hooft, R. *COLLECT, Data Collection Software*; Nonius BV: Delft, The Netherlands, 1998. (b) For DENZO, Data Collection and Processing Software, see: Otwinowski, Z.; Minor, W. In *Macromolecular Crystallography, Part A*; Carter, C. W., Sweet, R. M., Eds.; Methods in Enzymology 276; Academic Press: San Diego, CA, 1997; p 307. (c) Sheldrick, G. M. *SADABS, Program for Absorption Correction*; University of Göttingen: Göttingen, Germany, 1998.
(15) Frisch, M. J.; Trucks, G. W.; Schlegel, H. B.; Scuseria, G. E.; Robb, M. A.; Cheeseman, J. R.; Zakrzewski, V. G.; Montgomery, J. A., Jr.; Stratmann, R. E.; Burant, J. C.; Dapprich, S.; Millam, J. M.; Daniels, A. D.; Kudin, K. N.; Strain, M. C.; Farkas, O.; Tomasi, J.; Barone, V.; Cossi, M.; Cammi, R.; Mennucci, B.; Pomelli, C.; Adamo, C.; Clifford, S.; Ochterski, J.; Petersson, G. A.; Ayala, P. Y.; Cui, Q.; Morokuma, K.; Malick, D. K.; Rabuck, A. D.; Raghavachari, K.; Foresman, J. B.; Cioslowski, J.; Ortiz, J. V.; Baboul, A. G.; Stefanov, B. B.; Liu, G.; Liashenko, A.; Piskorz, P.; Komaromi, I.; Gomperts, R.; Martin, R. L.; Fox, D. J.; Keith, T.; Al-Laham, M. A.; Peng, C. Y.; Nanayakkara, A.; Gonzalez, C.; Challacombe, M.; Gill, P. M. W.; Johnson, B.; Chen, W.; Wong, M. W.; Andres, J. L.; Gonzalez, C.; Head-Gordon, M.; Replogle, E. S.; Pople, J. A. *Gaussian 98*, Revision A.7; Gaussian, Inc., Pittsburgh PA, 1998.
(16) Frisch, A.; Frisch, M. J. *Gaussian 98, User's Reference*, 2nd ed.; Gaussian, Inc., Pittsburgh, PA 15106, 1998.

Scheme 2. Drawing of the Isomers and Rotamers for $[Ru(CO)_2Cl_2(THZ)_2]$[a]

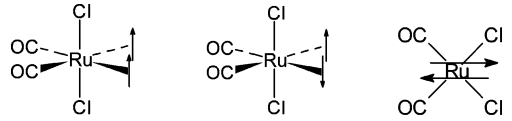

[a] The meaning of the arrow is the same as that reported in Scheme 1.

displacement 0.001 200 Å). The analysis of the Hessian showed no negative frequency for the optimized structures. Molecular drawings were obtained through the package GaussView03.[17]

Semiempirical. The structure optimization computations were performed through the HyperChem7.52 software package[18] at the ZINDO1 level.[19] The molecules investigated were *fac*-$[Ru(CO)_3Cl_2$-(THZ)]-A and -B (Scheme 1). Restraints were applied to fix the planarity of the THZ molecule and to fix the coordination sphere angles (to idealized values of 90° and 180°). The Ru−N−C5 bond angle was restrained to 127°.

Molecular Mechanics. Molecular mechanics analyses were performed by using an Amber-type force field implemented in MacroModel 5.0 package,[20] MMOD, running on a Silicon Graphics Indigo 2 machine. As regards the metal complexes, the coordination sphere was simulated by using an ad hoc force field obtained from this work and on a previous work on octahedral Ru(II) complexes.[21] The molecules were optimized up to rms 0.01 kcal, both at the gas phase and under the effect of a continuum field that simulates the presence of water.

A structure that simulates the copolymer CP2 was built via the molecular graphics options of MMOD including first a chain of 20 carbon atoms to which two $-C(=O)NHCH(COOH)C_6H_5$ side chains and 18 $-C(=O)NHCH(CH_3)CH_3$ side chains were linked; this fragment was linked via a $-C(=O)NHCH_2CH_2NHC(=O)-$ bridge to a twin fragment. The bridge was set almost at the middle of the two chains.

A total of four molecules were optimized: the tetraacid and -anionic forms both as isolated particles and particles in a continuum field simulating the solvent (water).

Subsequently, a molecular dynamics simulation with the default parameters of MMOD was performed and the lowest energy structure was again optimized via the Amber-type force field.

Behavior of 2 with Biomacromolecules. Behavior with Transferrin. A sample of 90 mg of HTF (M_w, 78 kDa)[22a,b] and 10 mg of $NaHCO_3$ in 10 mL of TRIS buffer (0.05 mol L^{-1}, HTF 1.15×10^{-4} mol L^{-1}) or phosphate buffer (NaH_2PO_4 and NaCl, both 0.05 mol L^{-1}) at pH 7.4 were stirred at 25 °C up to complete dissolution of protein. The UV spectrum for the solution was recorded after proper dilution with buffer. A sample of 10 mg of **2** was dissolved in 10 mL of TRIS buffer or phosphate buffer at 45 °C with stirring, and then the solution was cooled down to 25 °C. The solution of **2** was added to the freshly prepared solution of HTF and $NaHCO_3$ in such a way as to reach an Ru/HTF molar ratio in the range 1−400. The final mixture was stored at 25 or 37 °C for at least 2 h (mostly 24 h), and then 4 mL of the solution was ultrafiltered and the filtrate was analyzed through UV and AAS for the content of metal species.

Behavior with Albumin. A procedure similar to that just reported for THF was used for studies with bovine serum albumin (BSA, average M_w, 66.4 kDa).[22c]

Behavior with Calf Thymus DNA. The analysis of interaction of CT-DNA with **2** was performed by following ultrafiltration procedures similar to those described above for the interaction of the metal complex with HTF and BSA. The concentration of DNA was 6×10^{-5} mol L^{-1} and the Ru/DNA base pair molar ratio was $r = 0.1$, 0.5, 1, and 5 in the buffer. The Ru/DNA adducts were repeatedly ultrafiltered after 24-h incubation at 37 °C as described for the protein adducts. Circular dichroism (CD) spectra were recorded between 200 and 350 nm. ICP-OES measurements were performed on the upper and lower portions of the adduct at $r = 0.1$.

Absorption and Release of 2 from the Carrier Acryloyl−Polymer CP2. A freshly prepared fragment of CP2 was put on a porous microbasket, repeatedly rinsed with water, roughly dried with blotting paper, and then weighed. The basket was then soaked in freshly prepared TRIS buffer (0.05 mol L^{-1}, NaCl 0.100 mol L^{-1}, pH 7.4, 25 °C) solution that contained **2** (3×10^{-3} mol L^{-1}). The gel turned from colorless to yellow and then to orange with time. After 24 h of soaking, the loaded matrix was taken from the solution, rinsed with water, roughly dried via blotting paper, and then soaked in a TRIS buffer solution. The release of the metal complex was monitored via UV and AAS techniques up to 48 h.

Silica-Gel Matrix Dissolution Test. The dry gel (20 mg) was immersed into 50 mL of an aqueous solution that consisted of TRIS buffer (1×10^{-2} mol L^{-1}) and NaCl (0.150 mol L^{-1}) at pH 7.4 and 37 °C. The system was constantly stirred with a palette system at 60 rpm. At scheduled times, aliquots (1 mL) were removed for silica quantification and replaced with fresh buffer. Silica concentration was determined colorimetrically via the formation of the silico−molibdo complex.[23] Matrices were tested the day immediately after their preparation and after 2 months storage at room temperature in a sealed environment.

Results and Discussion

Synthesis of Ru−THZ Complexes. The one-pot reaction of high-purity commercially available $[Ru(CO)_3Cl_2]_2$, **1**, with thiazole in anhydrous ethanol at 55 °C for 2 h produced *fac*-$[Ru(CO)_3Cl_2(THZ)]$, **2**, that precipitated as large white crystals in high yields, upon cooling of the mother solution down to room temperature. The crystals were easily collected by filtration and they needed just to be washed with a small portion of cold ethanol and dried in the air for a few hours at room temperature. No further purification was needed; no host molecules are cocrystallized with the complex molecules, so no change in the composition occurred upon storage. The crystals do not react appreciably with the air atmosphere at 25 °C for periods of months. Visible light and Mo Kα X-radiation did not have any deleterious effect on the quality of the crystals for at least 1 week. The compound was stable up to 170 °C when slowly heated under a Kofler-type microscope. At the latter temperature it started melting and evolving gas. At 180 °C the crystals completely melt. A glassy material formed upon cooling.

(17) *GaussView3.0*; Gaussian, Inc., Pittsburg PA, 15106, 2003.
(18) *HyperChem*, Molecular Modelling System, Release 7.52 for Windows; Hypercube Inc., Gainsville, FL, 2005.
(19) *HyperChem, Reference Manual*; Hypercube Inc., Gainsville, FL, 2005, and references cited therein.
(20) Mohamadi, F.; Richards, N. G. J.; Guida, W. C.; Liskamp, R.; Lipton, M.; Caufield, C.; Chang, G.; Hendrickson, T.; Still, W. C. *J. Comput. Chem.* **1990**, *11*, 440.
(21) Pifferi, C.; Cini, R. *J. Chem. Soc. Dalton Trans.* **1998**, 2679.
(22) (a) Aisen, P.; Listowsky, I. *Annu. Rev. Biochem.* **1980**, *49*, 357. (b) Harris, W. R.; Wang, Z.; Brook, C.; Yang, B.; Islam, A. *Inorg. Chem.* **2003**, *42*, 5880. (c) Feng, R.; Konishi, Y.; Bell, A. W. *J. Am. Soc. Mass. Spectrosc.* **1991**, *2*, 387.
(23) Koroleff, F. In *Methods of Seawater Analysis;* Grasshoff, K. K., Ehrhardt, M., Ed.; Wiley-VCH: Weinheim, 1983; p 174.

Scheme 3. The Most Significant Steps of the Reaction That Produces **2** from **1** and THZ

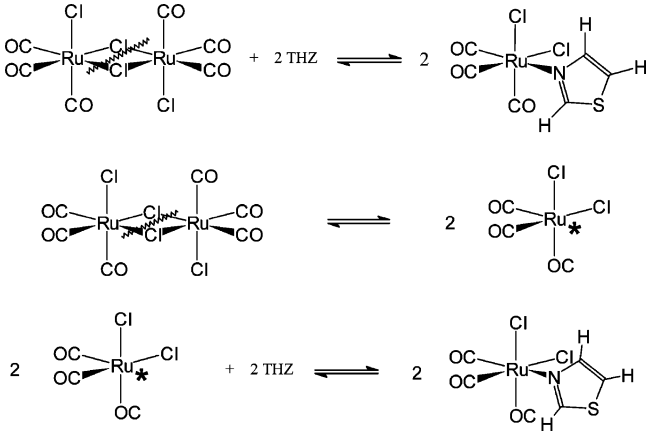

The mother solution that produced **2** gave yellow crystals of **3** on concentrating at room temperature.

The formation of **2** occurred through the reaction of the facial isomer *fac*-**1** (see isomer IIa in ref 4) with thiazole in a 1:2 molar ratio, as represented in eqs 1−3 and shown in Scheme 3:

$$fac\text{-}[Ru_2(CO)_6Cl_4] + 2THZ \rightleftharpoons 2fac\text{-}[Ru(CO)_3Cl_2(THZ)] \quad (1)$$

$$fac\text{-}[Ru_2(CO)_6Cl_4] \rightleftharpoons 2fac\text{-}[Ru^*(CO)_3Cl_2] \quad (2)$$

$$2fac\text{-}[Ru^*(CO)_3Cl_2] + 2THZ \rightleftharpoons 2fac\text{-}[Ru(CO)_3Cl_2(THZ)] \quad (3)$$

The reaction proceeds through the breakage of two Ru−Cl(bridge) bonds, transient formation of unsaturated Ru*, and subsequent attack of a THZ molecule on the free coordination sites of the two metal complex molecules.

It must be recalled that **3** precipitated when the concentration of free THZ was high with respect to Ru, in other words when much of Ru(II) was already separated from the mother solution in the form of **2** and when the volume of the solution was reduced by evaporation. It was found that increasing the excess THZ favored the formation of **3**. The same result was obtained by increasing the temperature of the mixture up to the boiling point of ethanol.

If isomer IIB of ref 4 is present in the starting material, its reaction with THZ produces **3** reasonably on the basis of the equations shown in Scheme 4.

The formation of **3** can reasonably be achieved through a cleavage of two bridging Ru−Cl bonds in a way to leave two Cl ligands trans to each other on each Ru center and a free coordination site trans to CO. This site can be occupied by a THZ molecule. Subsequently, a CO ligand trans to another CO is substituted by a second THZ molecule (this is made easy by the high trans influence and the effect from CO when compared to Cl). This results in the cis,trans,cis isomer.

However, it has to be noted that an analysis of the dimeric commercial product via infrared spectroscopy did not give any evidence for the presence of the mer isomer.[4] So, **3** forms via another pathway, or the mer isomer of **1** forms in the reaction mixture.

Scheme 4. Possible Pathways to the Formation **3** from the mer-isomer of **1**

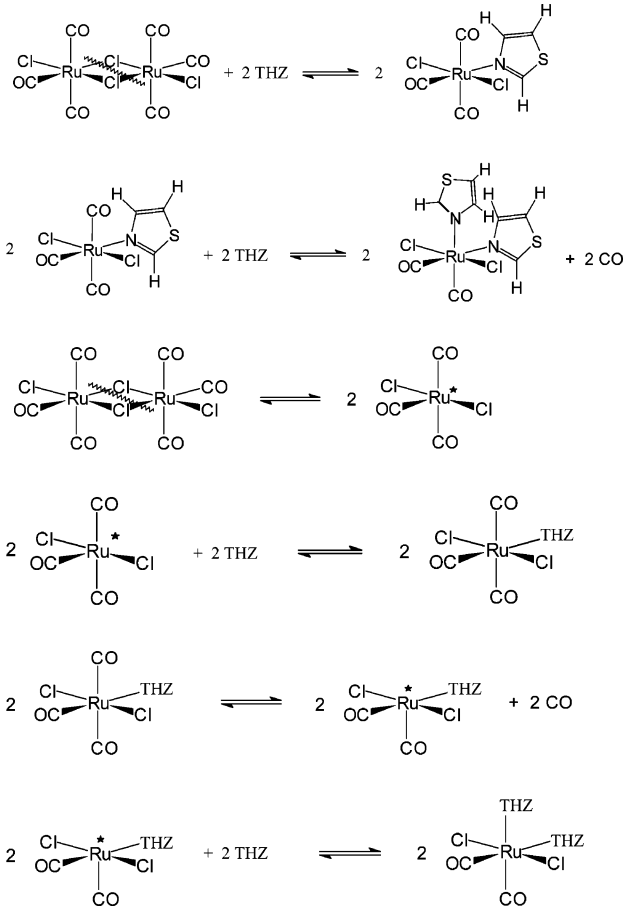

On assuming that *mer*-$[Ru_2(CO)_6Cl_4]$ forms in the reaction mixture and in case the cleavage of the Ru−Cl(bridge) bond for *mer*-$[Ru_2(CO)_6Cl_4]$ occurs on the bonds trans to terminal Cl (this is less probable because the smaller trans effect of Cl when compared to CO), *cis*,*cis*,*cis*-$[Ru(CO)_2Cl_2(THZ)_2]$ is formed.

The following equations (eqs 4−6) should explain the *fac*-$[Ru_2(CO)_6Cl_4]$/*mer*-$[Ru_2(CO)_6Cl_4]$ isomerization:

$$fac\text{-}[Ru_2(CO)_6Cl_4] \rightleftharpoons 2fac,cis\text{-}[Ru^*(CO)_3Cl_2] \quad (4)$$

$$2fac,cis\text{-}[Ru^*(CO)_3Cl_2] \rightleftharpoons 2mer,trans\text{-}[Ru^*(CO)_3Cl_2] \quad (5)$$

$$2mer,trans\text{-}[Ru^*(CO)_3Cl_2] \rightleftharpoons mer\text{-}[Ru_2(CO)_6Cl_4] \quad (6)$$

From *mer*-$[Ru_2(CO)_6Cl_4]$, the formation of *cis*,*trans*,*cis*- and *cis*,*cis*,*cis*-$[Ru(CO)_2Cl_2(THZ)_2]$ can reasonably be predicted as mentioned above. It has to be noted that the formation of *mer*,*trans*-$[Ru(CO)_3Cl_2(THZ)]$ was not revealed in the solid state via X-ray diffraction.

X-ray Structures. Structure of *fac*-[Ru(CO)$_3$Cl$_2$(THZ)] (2). The molecular structure of **2** is reported in Figure 1, whereas the selected bond lengths and angles are listed in Tables 2 and 3. Two complex molecules are present in the asymmetric unit. The two molecules have a pseudo-octahedral coordination geometry and differ as regards the orientation of the THZ ring plane with respect to the equatorial plane and are depicted as type-A and type-B in

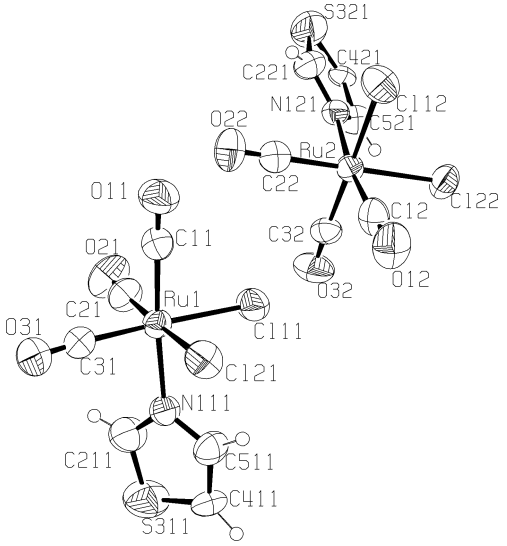

Figure 1. Ortep drawing of the two molecules of the asymmetric unit for **2**. Ellipsoids enclose 50% probability.

Table 2. Selected Bond Lengths (Å) for *fac*-[Ru(CO)$_3$Cl$_2$(THZ)] **2**

vector	length	vector	length
Ru(1)−C(31)	1.901(7)	Ru(2)−C(12)	1.909(7)
Ru(1)−C(21)	1.905(7)	Ru(2)−C(22)	1.898(7)
Ru(1)−C(11)	1.916(7)	Ru(2)−C(32)	1.907(7)
Ru(1)−N(111)	2.124(5)	Ru(2)−N(121)	2.121(5)
Ru(1)−Cl(11)	2.398(2)	Ru(2)−Cl(12)	2.404(2)
Ru(1)−Cl(21)	2.402(2)	Ru(2)−Cl(22)	2.401(2)
C(11)−O(11)	1.112(7)	C(12)−O(12)	1.115(8)
C(21)−O(21)	1.116(8)	C(22)−O(22)	1.128(7)
C(31)−O(31)	1.119(8)	C(32)−O(32)	1.121(7)

Table 3. Selected Bond Angles (deg) for *fac*-[Ru(CO)$_3$Cl$_2$(THZ)] **2**

vectors	angles	vectors	angles
C(31)−Ru(1)−C(21)	93.9(3)	C(22)−Ru(2)−C(12)	93.1(3)
C(31)−Ru(1)−C(11)	92.4(3)	C(22)−Ru(2)−C(32)	92.0(3)
C(21)−Ru(1)−C(11)	91.2(3)	C(12)−Ru(2)−C(32)	92.1(3)
C(31)−Ru(1)−N(111)	91.1(2)	C(22)−Ru(2)−N(121)	92.5(2)
C(21)−Ru(1)−N(111)	92.3(2)	C(12)−Ru(2)−N(121)	172.6(2)
C(11)−Ru(1)−N(111)	174.8(2)	C(32)−Ru(2)−N(121)	92.5(2)
C(31)−Ru(1)−Cl(11)	177.6(2)	C(22)−Ru(2)−Cl(22)	177.9(2)
C(21)−Ru(1)−Cl(11)	87.9(2)	C(12)−Ru(2)−Cl(22)	85.2(2)
C(11)−Ru(1)−Cl(11)	89.1(1)	C(32)−Ru(2)−Cl(22)	89.4(2)
N(111)−Ru(1)−Cl(11)	87.3(1)	N(121)−Ru(2)−Cl(22)	89.0(1)
C(31)−Ru(1)−Cl(21)	87.8(2)	C(22)−Ru(2)−Cl(12)	87.2(2)
C(21)−Ru(1)−Cl(21)	177.7(2)	C(12)−Ru(2)−Cl(12)	88.3(2)
C(11)−Ru(1)−Cl(21)	87.2(2)	C(32)−Ru(2)−Cl(12)	179.1(2)
N(111)−Ru(1)−Cl(21)	89.2(1)	N(121)−Ru(2)−Cl(12)	87.2(1)
Cl(11)−Ru(1)−Cl(21)	90.4(1)	Cl(22)−Ru(2)−Cl(12)	91.4(1)

Scheme 1. Three facial sites are occupied by carbonyl ligands and two cis sites are occupied by the chloride anions, whereas the sixth position is occupied by the nitrogen atom from thiazole. In one of the molecules, the projection of the THZ plane bisects the OC−Ru−CO and Cl−Ru−Cl angles, whereas in the second molecule the THZ plane bisects the two OC−Ru−Cl bond angles. The C5−N1−Ru−Cl torsion angles are −35.8(3)° and 37.9(3)°, respectively.

The four Ru−Cl bond distances average 2.401(2) Å and are in agreement with the values found for other *fac*-{Ru(CO)$_3$Cl$_2$} complexes.[24,25] The Ru−N vectors are trans to carbonyl ligands and their magnitude averages 2.124(5) Å. This value is higher than those found for *mer*-[RuCl$_3$(THZ)$_3$], where the nitrogen atoms are trans to chlorine or nitrogen atoms.[26] The Ru−N(THZ) vectors trans to N measure 2.106(5) and 2.082(5) Å, whereas the Ru−N bond trans to phosphorus is 2.183(5) Å for [RuCl$_2$(PPh$_3$)(THZ)$_3$].[21] The bond angles at Ru do not deviate much from the idealized values of 90° and 180°, the largest deviation being that for C2-Ru-C3, 2.5(3)°.

The C−O bond distances are in the range of 1.113(7)−1.128(7) Å and are in agreement with those previously found for several other Ru(II)−CO species; see, for example, *fac*-[Ru(CO)$_3$Cl$_2$(DMSO)] (DMSO, dimethyl sulfoxide).[5b] The values are also in perfect agreement with the structure of the CO molecule optimized at the ab initio coupled clusters level CCSD(T) (see computed structure below).

The thiazole ring for the two molecules of **2** is planar, the largest deviation from the plane defined by the endo-cyclic atoms being that relevant to C521, 0.025(7) Å. The N1−C5 bond distances are longer than the N1−C2 ones by 0.043(7) Å (average). The Ru−N−C21 and Ru−N−C51 bond angles are 125.0(5)° and 124.8(5)° (average), respectively.

Intramolecular Contacts. Intramolecular C−H···Cl and C−H···O hydrogen-bond-type interactions are present in the two complex molecules of **2**. For example, interactions involve C511 and Cl21 [C···Cl, 3.283(8) Å; C−H···Cl, 111.4(4)°], C221 and Cl12 [C···Cl, 3.281(7) Å; C−H···Cl, 101.2(4)°]; C211 and O21 [C···O, 3.806(9) Å; C−H···O, 114.9(6)°], and C221 and O22 [C···O, 3.804(9) Å; C−H···O, 117.9(6)°].

Intermolecular Contacts. Several intermolecular hydrogen-bond-type C−H···O and C−H···Cl interactions stabilize the crystal structure. Selected interactions involve C411 and O11 ($-x + 1$, $y - {}^1/_2$, $-z + {}^1/_2$) [C···O, 3.326(7) Å; C−H···O11, 156.1(4)°], C521 and O12 (x, $-y + {}^1/_2$, $z - {}^1/_2$) [C···O, 3.364(9) Å; C−H···O, 155.5(4)°], and C211 and Cl12 ($x - 1$, $-y + {}^1/_2$, $z - {}^1/_2$) [C···Cl, 3.400(7) Å; C−H···Cl, 143.5(5)°]. Interestingly, the oxygen atom from a CO ligand (namely O22) has a very short contact distance to a carbonyl ligand from the other complex molecule [O22···O11, 3.131(6) Å; O22···C11, 3.377(6) Å]. In a similar fashion, a chlorine ligand of the first complex molecule (Cl11) has a short contact with the C32−O32 carbonyl ligand of the other complex molecule [Cl···O, 3.578(5) Å; Cl···C, 3.514(6) Å]. These latter contacts suggest the presence of weak Lp···π interactions that involve the lone pair electrons of Cl and O atoms and the π electrons of the carbonyl ligand. Weak stacking interactions between thiazole rings also occur. For example, the rings related by an inversion center ($-x + 2$, $-y + 1$, $-z$) stack [N121···C421, 3.741(7) Å].

Structure of *cis,trans,cis*-[Ru(CO)$_2$Cl$_2$(THZ)$_2$] (3). Results from the Data Set Collected at 293 K. The molecular structure of **3** is represented in Figure 2, whereas the values of the bond distances and bond angles are reported in Tables 4 and 5.

The metal center is located on a 2-fold axis that bisects the N−Ru−N and the C−Ru−C bond angles. Furthermore,

(24) Gray, G. M.; Duffey, C. H. *Acta Crystallogr.* **1996**, *C52*, 861.
(25) Bergmeister, III, J. J.; Hanson, B. E.; Merola, J. S. *Inorg. Chem.* **1990**, *29*, 4831.
(26) Pifferi, C.; Cini, R. *Acta Crystallogr.* **2000**, *C56*, 439.

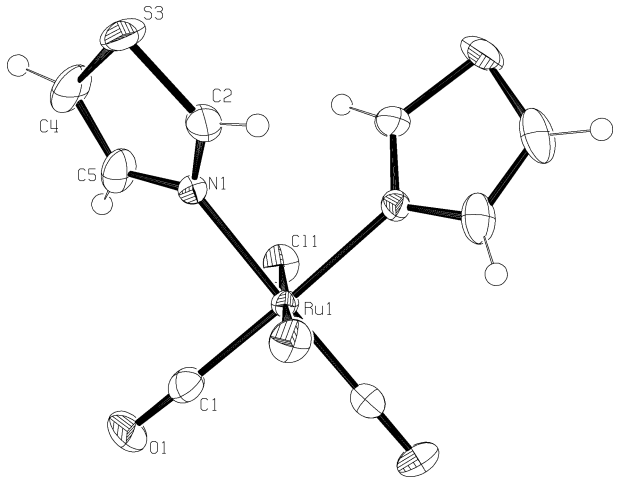

Figure 2. Ortep drawing of the molecule of **3** (data collection at 120 K). Ellipsoids enclose 50% probability. Only one of the two orientations of the thiazole ligand is represented; similarly, only the CO and Cl ligands with the highest occupancy are represented, for clarity.

Table 4. Bond Lengths (Å) for *cis*,*trans*,*cis*-[$Ru(CO)_2Cl_2(THZ)_2$] **3**

	length	
vector	293 K	120 K
Ru(1)−C(1)	1.919(4)	1.878(8)
Ru(1)−C(1)		1.889(10)
Ru(1)−N(1)	2.144(3)	2.128(2)
Ru(1)−Cl(1)	2.389(1)	2.375(1)
Ru(1)−Cl(1)		2.337(9)
C(1)−O(1)	1.053(5)	1.134(8)
C(1)−O(1)		1.112(10)
N(1)−C(5)	1.326(4)	1.336(3)
N(1)−C(2)	1.343(5)	1.349(3)

Table 5. Selected Bond Angles (deg) for *cis*,*trans*,*cis*-[$Ru(CO)_2Cl_2(THZ)_2$] **3**[a]

	angles	
vectors	293 K	120 K
C(1)−Ru(1)−N(1)	91.9(1)	92.2(3)
N(1)−Ru(1)−Cl(1)	89.8(1)	89.5(1)
Cl(1)#1−Ru(1)−Cl(1)	177.3(1)	176.9(1)
N(1)−Ru(1)−N(1)#1	86.0(1)	86.1(1)
C(1)#1−Ru(1)−C(1)	90.2(2)	89.5(7)

[a] Symmetry transformations used to generate equivalent atoms: #1, $-x+1, y, -z+1/2$.

the molecule is affected by a severe statistical disorder. In fact, the data set collected at 293 K reveals a disorder for the thiazole molecules. The disorder could be solved by taking into account two possible orientations that simulate a 2-fold axis along each Ru−N vector. The coordination sphere is pseudo-octahedral, with two *cis*-thiazole ligands and two *cis*-carbonyl ligands in the equatorial plane: the apical positions are occupied by the two chloride anions. The refined structure has Ru−Cl bond distances [2.389(1) Å] slightly shorter than the values found for **2**. The Ru−N and Ru−C bond lengths [2.144(3) and 1.919(4) Å] are in agreement with the values for **2**. Notwithstanding, it has to be pointed out that the C−O bond distances are unusually short [1.053(5) Å]. Several structures that contain metal−carbonyl functions, as deposited at the Cambridge Crystallographic Data Base,[27] have C−O bond lengths as short as those found in the present work (47 structures). Most of the related papers do not have any comment on that anomaly (see, for example, ref 28). We thought that the short C−O bond could possibly be explained on the basis of some occupational disorder for chloride and carbonyl ligands. This hypothesis was considered worthy of further investigation for **3**, and collection of X-ray diffraction data at low temperature and through a higher energy beam was planned and performed (see Experimental Section).

Results from the Data Set Collected at 120 K. The statistical disorder of the THZ ring around the Ru−N vector was solved with the model described just above for the data set collected at 293 K. The Ru−N bond distance is 2.128(2) Å, in nice agreement with the values found for **2** and for **3** at 293 K.

Furthermore, the careful analysis of the difference Fourier map at a certain stage of refinement after the Cl, O, N and C atoms were located showed that around the carbonyl ligand a residual electron density was still present, and the same happened around the chloride ligand. The disorder relevant to the carbonyl and chloride sites that was predicted during the previous refinement was then confirmed at low temperature. The carbonyl ligands have an occupancy of 88%, the remaining 12% being chloride anion; the opposite happens for the chloride positions that have occupancy of 88%, where the remaining 12% is carbonyl. The analysis was assumed as correct and the bond lengths and angles fit the expectations much better. The Ru−C bond distance is 1.878(8) Å; the Ru−Cl bond distance is 2.375(1) Å, in agreement with the values of **2**; finally, the C−O bond length 1.134(8) Å is in perfect agreement with the values for **2**, with other data from X-ray diffraction experiments, and with theory. The Ru−C−O bond angle was freely refined and converged to 176.9(1)°.

Weak Interactions. Intramolecular hydrogen-bond-type interactions occur between C5 and Cl1 [C···Cl, 3.390(5) Å; C−H···Cl, 101.0(3)°], whereas intermolecular H-bonds occur between C2 and O1 ($x+1/2, y+1/2, z$) [C···O, 3.379(7) Å; C−H···O, 128.9(4)°] and between C5 and Cl1 ($-x, y, z-1/2$) [C···Cl, 3.554(3) Å; C−H···Cl1, 139.6(6)°]. Stacking-type interactions occur between THZ rings. The shortest stacking distance is that of C5 and C4′ ($-x+1/2, -y+1/2, -z+1$), 3.627(6) Å.

Computed Structures. Ab Initio and DFT. CO. The carbon monoxide molecule as optimized at the CCSD(T)/6-311++G** level has a bond distance of 1.137 Å, in perfect agreement with the values found in the solid state for **2** and **3**. It has to be noted that the CO molecule as computed at the hybrid density functional B3LYP/6-31+G* level has the same bond distance, 1.137 Å.

[$Ru(CO)_3Cl_2(THZ)$]. The optimized structures for *fac*-[$Ru(CO)_3Cl_2(NH_3)$] and *fac*-[$Ru(CO)_3Cl_2(THZ)$] performed at the B3LYP/(Lanl2DZ, Ru; 6-31G, CHNOSCl) level have

(27) The Cambridge Crystallographic Data Center. *The Cambridge Crystallographic Data Base*, Version 5.24; November 2004.
(28) Haukka, M.; Kiviaho, J.; Ahlgren, M.; Pakkanen, T. A. *Organometallics* **1995**, *14*, 825.

Ru−Cl bond distances 2.483 and 2.452 Å, respectively. The computed Ru−N bond lengths are 2.160 and 2.152 Å, whereas the average Ru−C bond distances are 1.920 Å. The comparative analysis with the experimental values for **2** shows a somewhat overestimation for Ru−Cl by theory. Even the C−O distances (range 1.165−1.171 Å for computed and 1.113−1.128 Å from X-ray for **2**) are significantly overestimated by theory. In the case where the basis set is improved and the level of theory is B3LYP/(Lanl2DZ, Ru; 6-31+G*, CHNOSCl), the agreement between computed and experimental parameters is better for the C−O bond distances (range 1.137−1.142 Å for both the ammino and thiazole derivatives). Even the Ru−Cl bond distances are better reproduced with the improved basis set. The bond distances for the thiazole ring are well-reproduced by both the basis sets. The computations at B3LYP/(Lanl2DZ, Ru; 6-311++G**, CHNOSCl) did not change things much and Ru−Cl, Ru−C, Ru−N, and C−O bond distances are 2.448, 1.934, 2.186 (C2H is *syn* to CO), and 1.134 Å, respectively. The computed bond angles are in perfect agreement with those determined for the solid-state structures. All the refinements were done without any restraints. The optimized structure has a C2−N−Ru−Cl torsion angle of 134.6°, which compares well with that found at the solid state for **2** (146.4°). In the case where the starting structure for the optimization procedure has C2−N−Ru−Cl of −30° (i.e., the complex is type-A, Scheme 1), the optimized structure has a value of −31.5° for the same torsion angle (it maintains the same conformation).

The total electronic energy for the two optimized structures for the THZ derivative at the B3LYP/(Lanl2DZ, Ru; 6-311++G**, CHNOSCl) level is −645.114 27 and −645.115 85 hartrees (difference, 0.990 kcal mol^{-1}), which compares well with the equioccupancy of the two rotamers at the solid state.

Frequencies. The computed frequencies for the C−O stretching vibrations (B3LYP/Lanl2DZ, Ru; 6-31G, CHNOSCl) are 1985.7 cm^{-1} (30.9850 mdyn $Å^{-1}$, 661.3817 km mol^{-1}), 2012.9 cm^{-1} (31.8142 mdyn $Å^{-1}$, 644.1234 km mol^{-1}), and 2075.4 cm^{-1} (33.7077 mdyn $Å^{-1}$, 502.2129 km mol^{-1}). The values compare well with those found experimentally (see IR spectroscopy above). However, on improving the basis set (6-311++G**, CHNOSCl), the agreement becomes better: calcd 2107.3 cm^{-1} (35.0277 mdyn $Å^{-1}$, 672.7024 km mol^{-1}), 2133.7 cm^{-1} (35.8701 mdyn $Å^{-1}$, 647.3468 km mol^{-1}) and 2194.0 cm^{-1} (37.8082 mdyn $Å^{-1}$, 543.6959 km mol^{-1}); found (CH_2Cl_2), 2048, 2073, 2135 cm^{-1}. It has to be noted that overestimation by theory is accepted in the literature and that the correction factor from this work, 0.972, is in agreement with the values reported in ref 16.

[Ru(CO)$_2$Cl$_2$(THZ)$_2$]. The optimized structures for *cis,trans,cis*-[Ru(CO)$_2$Cl$_2$(NH$_3$)$_2$] and *cis,trans,cis*-[Ru(CO)$_2$Cl$_2$(THZ)$_2$] were computed by using the same strategies for those just reported above for the *fac*-{Ru(CO)$_3$} derivative (whereas the choice of the basis set was based on criteria of both accuracy of results and reduction of computational time). The optimized structure for the *cis,trans,cis* isomer at B3LYP/(Lanl2DZ, Ru; 6-311++G**, CHNOSCl) has

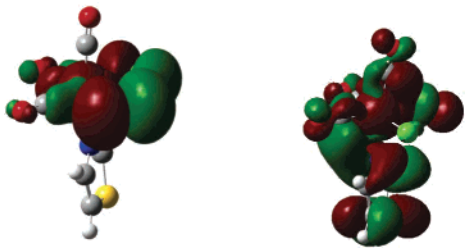

Figure 3. HOMO (left) and LUMO (right) for *fac*-**2**-A (see Scheme 1).

Ru−Cl, Ru−C, Ru−N, and C−O bond distances of 2.473, 1.898, 2.226, and 1.139 Å, respectively. Because of the disorder found at the solid state for **3**, the comparative analysis of bonding parameters between theory and experiment is not worthy of efforts. The structures of *cis,trans,cis*- and *cis,cis,trans*-[Ru(CO)$_2$Cl$_2$(THZ)$_2$] optimized at the same level of theory have total electronic energies of −712.80437 and −712.79398 (difference, 6.52 kcal mol^{-1}), in agreement with the X-ray structure for **3** that shows a preponderance of the *cis,trans,cis* isomer (see above).

Molecular Orbitals. The analysis of the MOs for *fac*-**2**-A shows that the HOMO is composed mostly by metal, equatorial carbonyl, and chloride atomic orbitals (Figure 3), whereas the LUMO consists mainly of atomic orbitals from thiazole atoms, even though metal and carbonyl atomic orbitals are significantly involved as well. Electron excitation from HOMO to LUMO corresponds therefore to a charge transfer from the {Ru(CO)$_2$Cl$_2$} equatorial system to thiazole and apical carbonyl.

Semiempirical, ZINDO/1. The structure for *fac*-[Ru(CO)$_3$Cl$_2$(THZ)] was optimized at the semiempirical level to check the reliability of this fast, easily accessible computational tool for these types of complex molecules. Four rotamers that differ for the orientation of the THZ plane with respect to the *cis,cis*-{Ru(CO)$_2$Cl$_2$} equatorial system went to convergence (rms < 0.01 kcal). Two of the rotamers are type-B and their total electronic energy is −4653.1 kcal (Cl1/Cl2-Ru−N−C2, 26°). The other two rotamers are almost type-A but close to an eclipsed conformation as regards the THZ plane projection and Cl−Ru−C lines. The electronic energy is −4651.4 kcal. So, the results are comparable to those from DFT calculation, even though the agreement with experiment as regards the bond distances is much poorer for the semiempirical level than for DFT (i.e., the Ru−N length is underestimated by 0.17 Å with respect to the X-ray diffraction).

Molecular Mechanics, Amber-type Force Field. Modeling the Structure for CP2 Polymer. The optimized model for the CP2 polymer (see above computational methods) has four carboxylate groups that mostly extend outward from the molecule and are involved in hydrogen bonds mostly to NH-amide groups. A linear fragment of the optimized model for the polymer is represented in Figure 4. Coordination residues like *fac*-{Ru(CO)$_3$(OH)(THZ)} that possibly approach the oligomer have enough room to link the carboxylate groups in a mono- or even bidentate fashion.

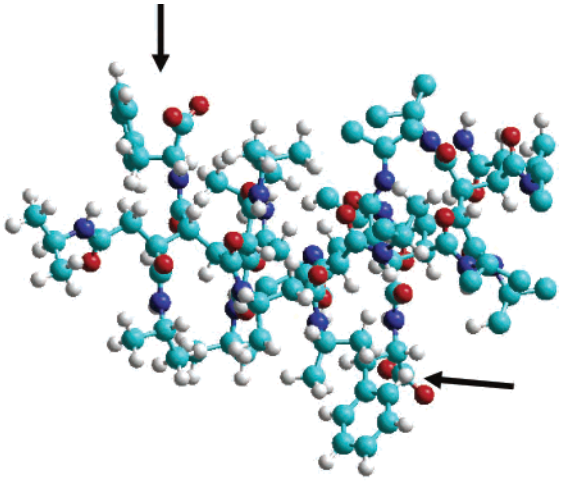

Figure 4. Representation of an oligomer from the geometry-optimized structure (molecular mechanics) for the model of the hydrogel poly(*N*-acryloyl-L-phenylalanine-*co*-*N*-isopropylacrylamide) in the cross-linked form, CP2, that was used as carrier for the ruthenium species. The two carboxylate groups from the phenylalanine moieties are marked by arrows.

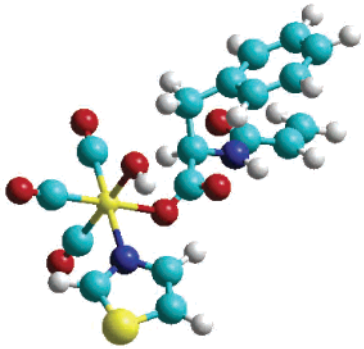

Figure 5. Optimized structure for *fac*-[Ru(CO)$_3$(OH)(PHE)(THZ)] through the methods of molecular mechanics.

Modeling the Structure of *fac*-[Ru(CO)$_3$(OH)(PHE)(THZ)]. The optimized minimum energy structure for the complex molecule (Figure 5, Table 6) has monodentate PHE anionic ligand in a bent arrangement. This conformation for the ligand allows an unhindered coordination of the metal center. No unacceptable short intramolecular contact between PHE atoms and the coordination residue is detectable. It is reasonable to assume that the PHE-{Ru(CO)$_3$(OH)(THZ)} systems in the CP2 carrier loaded by *fac*-[Ru(CO)$_3$(H$_2$O)-(THZ)]$^{2+}$ have a structure similar to that optimized for *fac*-[Ru(CO)$_3$(OH)(PHE)(THZ)].

Reaction of 2 with Water. Compound **2** is appreciably soluble at 25 °C in water and significantly soluble in several other solvents: methanol, ethanol, dichloromethane, chloroform, dimethyl sulfoxide. On the contrary, **3**, while not significantly soluble in water, is soluble in all the organic solvents just mentioned.

UV. The spectrum of freshly prepared solutions of **2** in anhydrous methanol (8.9×10^{-5} mol L^{-1}) at 25 °C has a peak at 230 nm (ϵ, 8500 cm^{-1} mol^{-1} L) and a clear shoulder at 276 nm (1900 cm^{-1} mol^{-1} L). On adding a small amount of water (three drops to 10 mL), the spectrum changes slowly as pictured in Figure 6. After ca. 6 h the original peak at 230 nm changes to a shoulder, and the original shoulder at ca. 267 decreases in absorbance and shifts toward red. The overlap of the peaks shows an isosbestic point at 300 nm. Upon addition of water to a solution of **2** in methanol at 37 °C the effects just described for the UV spectrum at 25 °C have the same trend but equilibration is achieved more rapidly.

Table 6. Selected Amber-type Force Field Parameters Optimized in This Work To Compute the Structure of *fac*-[Ru(CO)$_3$(OH)(PHE)(THZ)][a]

bond	R_o (Å)	K^b (kcal Å^{-2} mol^{-1})
Ru−C	1.95	250
Ru−N	2.18	120
Ru−O	1.98	120

angle	θ_o (deg)	K^θ (kcal rad^{-2} mol^{-1})
C−Ru−C	90.0	50
C−Ru−N	90.0	40
C−Ru−O	90.0/180.0	50/60
N−Ru−O	90.0	50
Ru−C−O	180.0	70
Ru−N−C	120.0	50
Ru−O−C	109.0	60

torsion terms	V1 (kcal mol^{-1})	V2 (kcal mol^{-1})	V3 (kcal mol^{-1})
Ru−N(sp^2)*C(sp^2)*C(sp^2)	0.0	1.5	0.0
Ru−O0*C(sp^2)*00	0.0	0.0	0.0
00*Ru*00*00	0.0	0.0	0.0

[a] The parameters relevant to PHE and THZ moieties are those implemented in the MMOD software package.[20]

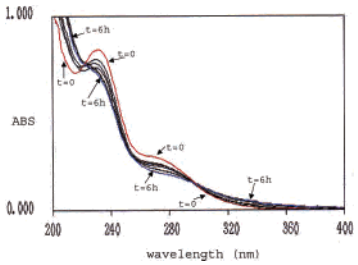

Figure 6. Superimposition of the UV spectra of **2** in anhydrous methanol (8.9×10^{-5} mol L^{-1}, 25 °C; freshly prepared, $t = 0$) and after the addition of 75 mg of H$_2$O to 10 mL of solution, as recorded at a time interval of 70 min and finally recorded 6 h after the addition of water ($t = 6$ h).

The spectrum of **3** in methanol has a peak at 235 nm (10 910 cm^{-1} mol^{-1} L) but no appreciable shoulder at 267 nm. Rather, a new weak absorption band is observed in the near-UV at 370 nm (441 cm^{-1} mol^{-1} L). On adding a small amount of water to the methanol solution, no significant change occurs up to 24 h.

The data for **2** are interpreted in terms of the aquation equilibria (see eq 7).

$$fac\text{-}[Ru(CO)_3Cl_2(THZ)] + 2H_2O \rightleftharpoons fac\text{-}[Ru(CO)_3(H_2O)_2(THZ)]^{2+} + 2Cl^- \quad (7)$$

In aqueous solution the formation of the dihydroxo species is predicted, depending on pH (eqs 8 and 9).

$$fac\text{-}[Ru(CO)_3(H_2O)_2(THZ)]^{2+} + H_2O \rightleftharpoons fac\text{-}[Ru(CO)_3(H_2O)(OH)(THZ)]^{+} + H_3O^{+} \quad (8)$$

$$fac\text{-}[Ru(CO)_3(H_2O)(OH)(THZ)]^+ + H_2O \rightleftharpoons fac\text{-}[Ru(CO)_3(OH)_2(THZ)] + H_3O^+ \quad (9)$$

The pH values (25 °C) of an acidified (HCl) aqueous solution of **2** as a function of added NaOH are reported in Figure 7. Two titration steps are evident from the curve, and approximate values of pK_{a1} and pK_{a2} can be estimated at 3.0 and 6.5, respectively. The latter value could be refined through least-squares methods by using the Hyperquad software package[29] and converged to 6.80(5). At pH 7.4, both the H_2O ligands are therefore in the hydroxo form; i.e., the prevailing species is *fac*-$[Ru(CO)_3(OH)_2(THZ)]$. Owing to the well-known bridging ability of OH^-, the formation of dimer *fac*-$[Ru(CO)_3(OH)(THZ)]_2$ is possible. The data for **3** were interpreted with the absence of aquation equilibria, in agreement with the structure of the molecule that has the two chloride atoms *trans* to each other, so they do not experience the high *trans* influence from carbonyl when compared to **2**. In the case where **2** is dissolved in TRIS buffer, the solution becomes yellowish at least under aerobic conditions. It is reasonable that the aqua species react slowly with triethanol-amine. No evidence of sensitivity of **2** to the visible radiation was observed both in the solid state and in solution.

^{1}H NMR. The spectrum of free THZ in D_2O has peaks at 8.82 ppm (H2, 1H, large doublet), 7.75 ppm (H4, 1H, doublet), and 7.45 ppm (H5, 1H, multiplet). The assignment is confirmed by the COSY spectrum from the same solution. The spectrum of **2** in D_2O solution changes significantly with time up to complete dissolution. Immediately after the mixing of **2** and D_2O the spectrum has only one signal, attributable to H_2O at 4.64 ppm. After 0.5 h (25 °C), a series of peaks appears in the region 9.42−7.9 ppm. The intensity of the peaks around 7.9 ppm is almost twice that of the peaks around 9.4 ppm. The peaks of each group do not have the same intensity. The group around 9.4 ppm consists of three major peaks whose area ratio is 1.3:1:1.1 at 9.42, 9.28, and 9.11 ppm, respectively. Two other peaks at 9.71 and 8.92 ppm have relative intensities of 0.7 and 0.6, respectively. All the signals at ca. 9.4 ppm are attributed to the H2 proton of ruthenium-bound THZ in different species. In fact, no signal can be attributed to free THZ. The three major components are tentatively attributed to **2**, *fac*-$[Ru(CO)_3Cl(OH_2)(THZ)]^+$, *fac*-$[Ru(CO)_3(OH_2)_2(THZ)]^{2+}$. The two smaller peaks may originate from *mer*-$Ru(CO)_3$, *cis*-$Ru(CO)_2$ derivatives, or from binuclear species. The peaks around 7.9 ppm are attributed to H4 and H5 protons of ruthenium-bound THZ.

Conductivity. Conductivity measurements were performed in a solution of **2** in methanol (4 mL)/water (0.8 mL). The conductivity increased with time and reached a plateau after ca. 2 h. The average value of conductivity was 153 Ω^{-1} cm^2 mol^{-1}, a value that compares well with those reported for electrolytes of the type $A^{2+}2B^-$ on the basis of the study by Geary.[30] These data confirm the aquation processes reported above. It has to be noted that in highly alcoholic media the Ru-bound water molecules are mostly not deprotonated.

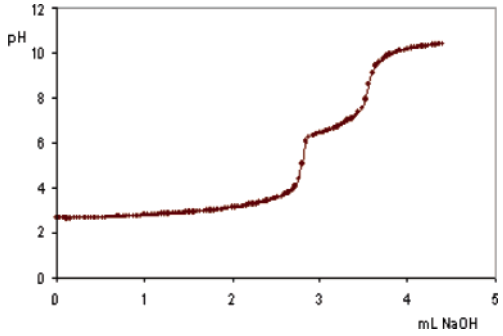

Figure 7. Potentiometric titrations of aqueous solutions of **2** with NaOH.

Behavior of 2 with Biomacromolecules. The preliminary study of reactivity of **2** with biomacromolecules had the limited goal to estimate the gross behavior of the metal complex toward two selected serum proteins (namely, human apotransferrin and bovine serum albumin) and CT-DNA.

Bovine serum albumin (BSA) and human Apotransferrin (HTF). The indirect measurements of binding of **2** to the proteins as carried out via ultrafiltration through filters with cutoff at 10 kDa (from phosphate and TRIS buffered solutions) showed that very modest amounts of ruthenium complex passed down into the filtrate (as determined via ICP and UV spectroscopy), implying that substantial ruthenium interaction to the two proteins takes place.[2g] The amount of ruthenium in the lower fraction was 5 ± 2% and 15 ± 3% for BSA and HTF, respectively. In the case of HTF, even if the Ru/protein molar ratio is as high as 20:1 the percentage of ruthenium in the filtrate is 18 ± 3%. The behavior of **2** with BSA and HTF is explained by taking into account the affinity of the complex toward the carboxylate functions (see synthesis above and reaction with carboxylate below). It has to be noted that HTF and BSA have tens of carboxylates at the external surface and most of them are accessible to attack from the *fac*-$\{Ru(CO)_3(THZ)\}$ coordination residue (see, for example, the structure of a HTF protein with PDB code 1D3K).[31] Further work should be done to help in discriminating between specific and nonspecific metal binding to the proteins.

Calf Thymus DNA. Ultrafiltration experiments showed 86 ± 4% ruthenium complex in the filtrate when the Ru/base pair molar ratio is 1:10. It is clear that the binding of ruthenium to DNA is less pronounced than the corresponding one to the proteins. The CD spectra of CT-DNA in the UV region recorded with increasing amounts of **2** showed that the effect of the metal complex on the characteristic bands of B-type DNA is minimal up to a Ru/base pair molar ratio of 1 (Figure 8). At high molar ratios (r = 5), spectral

(29) (a) Gans, P.; Sabatini, A.; Vacca, A. *Hyperquad 2003*—Equilibrium Constants from pH and/or Absorbance Data; Protonic Software and University of Florence, Florence, 2003.

(30) Geary, W. J. *Coord. Chem. Rev.* **1971**, *7*, 81.

(31) (a) Berman, H. M.; Westbrook, J.; Feng, Z.; Gilliland, G.; Bhat, T. N.; Weissig, H.; Shindyalov, I. N.; Bourne, P. E. The Protein Data Bank. *Nucleic Acids Res.* **2000**, *28*, 235. (b) Yang, A. H.; MacGillivray, R. T.; Chen, J.; Luo, Y.; Wang, Y.; Brayer, G. D.; Mason, A. B.; Woodworth, R. C.; Murphy, M. E. *Protein Sci.* **2000**, *9*, 49.

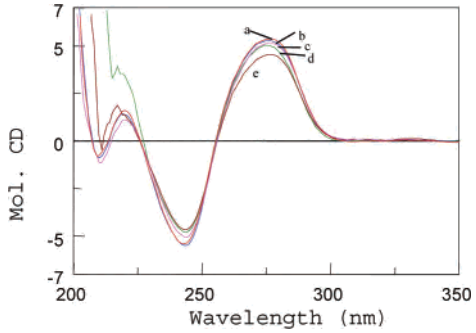

Figure 8. CD spectra of solutions that contain **2** and CT-DNA in phosphate buffer (0.01 mol L^{-1}), NaCl (0.020 mol L^{-1}), pH 7.5: (a) CT-DNA (6×10^{-5} mol L^{-1}) and **2**/DNA base pair (b) $r = 0.1$, (c) $r = 0.5$, (d) $r = 1$, (e) $r = 5$.

alterations of the CD spectrum were noted, consisting of ca. 15% loss in intensity of both bands at 240 and 270 nm.

Reactivity of 2 with Guanosine 5′-Monophosphate. The ^{1}H NMR spectrum of **2** in D_2O (0.03 mol L^{-1}) is significantly influenced by the addition of Na_2GMP (1:1 molar ratio). Three minutes after the dissolution of GMP into **2**/D_2O the solution became pale yellow. After 15 min, the spectrum had significant changes in the region around 9.4 ppm with respect to the spectrum of **2** in D_2O. The five peaks in the NMR spectrum of the D_2O solution of **2** alone where no longer present in the spectrum of the mixture that contained **2** and GMP; two peaks at 8.85 and 8.90 ppm appeared. This is the region for the signals of the THZ-H2 proton, and the data suggest the presence of two magnetically distinct GMP ligand molecules. It is probable that two different Ru-GMP species formed. The signal for H8 was shifted 0.11 ppm upfield with respect to that of free GMP in D_2O. Free THZ was not observed in the spectrum of **2**/GMP/D_2O. Twenty-four hours after mixing the spectrum did not change significantly. It has to be noted that an orange precipitate formed and the mother liquor was orange, too. The p*D* of the suspension is ca. 5. These data suggest that GMP reacts quickly with *fac*-[$Ru(CO)_3(H_2O)_2(THZ)$]$^{2+}$ in aqueous solution, via interaction of ruthenium with the phosphate from GMP. This interaction does not remove THZ from the coordination sphere.

Adsorption and Delivery of 2 by CP2 Polymer and Reaction with Carboxylate. *fac*-{$Ru(CO)_3$(THZ)}−CP2 Adduct. Compound **2** was absorbed by CP2 when the hydrogel was soaked into a TRIS buffer solution that contained a relatively high concentration of ruthenium species. The release of metal species from CP2 into a fresh TRIS buffer solution, at 25 °C, as monitored via UV spectroscopy is represented in Figure 9. It has to be recalled that CP2 has active carboxylate functions accessible to attack from the metal residue.

***fac*-{$Ru(CO)_3$(THZ)}−Carboxylate Adduct.** With the aim to study the reactivity of the hydrogel with the ruthenium complexes, low molecular weight carboxylic acids were selected as models, and their reactivity with the ruthenium species was studied. HPHE reacted with **2** in aqueous media at room temperature to produce a solid compound that was isolated and characterized via elemental analysis; ^{1}H NMR, UV, and IR spectroscopy; and molecular mechanics analysis.

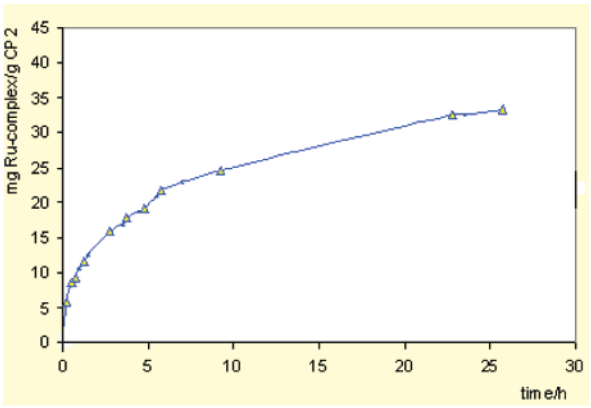

Figure 9. Release of **2** from the CP2/**2** system into TRIS buffer at pH 7.4 as represented by the absorbance values at 230 nm in the time period 0−26 h from the beginning of soaking of the embedded hydrogel in the buffer.

The compound can be formulated as *fac*-[$Ru(CO)_3$(OH)-(PHE)(THZ)]·H_2O, **6** (see Figure 5). The coordination sphere is pseudo-octahedral, and the three carbonyl and the thiazole ligands are not removed by the reaction of **2** with PHE. The two *cis*-positions occupied by the chloride anions in **2** are substituted by an oxygen atom from the carboxylate group from PHE and by an hydroxo ligand. The structure of the benzoate derivative is predictably similar to that of the PHE one, at least as regards the coordination sphere and coordination mode of the COO^- function.

Absorption and Delivery of 2 by Synthetic Silica Gel. The silica gel was prepared in the presence of **2** in CH_3OH/C_2H_5OH in such a way as to produce a material that contained ca. 5% w/w of the metal complex (see Experimental Section). The silica gel/ruthenium species system was separated from the mother maturation liquor through filtration and then dried at 50 °C up to constant weight (ca. 24 h). The release of total ruthenium from silica gel in TRIS/NaCl buffer as evaluated via AAS showed that ca. 2 mg L^{-1} Ru were delivered within 18 h. The release of metal as a function of time has the same trend as the release of SiO_2 from the gel. This suggests that the release itself happens after erosion of the matrix and not through diffusive processes.[32] Interestingly, the erosion of the gel that contains the ruthenium species is 10 times faster than that of the free gel or gel that contains conventional organic pharmaceutical compounds. A reasonable explanation is that some linkage between the silicate tetrahedron and the metal species occurs, and this interaction makes the erosion of the matrix easier.

Conclusion

A new ruthenium compound that is appreciably soluble in aqueous systems was prepared and fully structurally characterized at the solid state and in solution. Its molecule has two *cis*-chloride donors that are easily removed by water or other ligands in aqueous media. The labile coordination sites can be occupied by carboxylate or silicate anions and through this the ruthenium complex is adsorbed by silica gels and organic hydrogels that contain carboxylate residues.

(32) Kortesuo, P.; Ahola, M.; Karlsson, S.; Yli-Urpo, I.; Kiesvaara, J. *Biomaterials* **2000**, *21*, 193.

Because of the chemical liability, the linkages are reversible and the *fac*-{$Ru(CO)_3(THZ)$}$^{2+}$ coordination residue is released from the carriers in aqueous media under certain conditions of temperature and ionic strength. This opens an interesting perspective for administering molecule **2** in the case it has pharmacological activity. Synthetic hydrogels can in principle be implanted in specific tissues that need a controlled flux of the active species after being loaded with the metal compound. *fac*-{$Ru(CO)_3(THZ)$} is able to link to at least two serum proteins by which it can be transported in living tissues.

Biological studies devoted to investigate cytotoxic activity against a large panel of cancer cells in vitro and anticancer and antimetastases activity in vivo are recommended for compound **2** and for homologous ruthenium derivatives with other ligands instead of THZ. It has to be noted that well-known NAMI-A has good antimetastases and anticancer activity, even though its cytotoxic activity in vitro is low.

Studies aimed to further investigate the reactivity of **2** and its analogous with biomacromolecules have to be carried out carefully in future works.

Acknowledgment. Ministero dell'Università e della Ricerca Scientifica e Tecnologica (MURST, Rome) and University of Siena (Unisi) are gratefully acknowledged for funding through the programs PRIN 2004 and PAR 2004, respectively. R.C. gratefully acknowledges the X-ray crystallography group at the School of Chemistry, University of Southampton, Southampton, UK. G.T. thanks Consorzio Inter-universitario di Ricerca in Chimica dei Metalli nei Sistemi Biologici (CIRCMSB, Bari, year 2003). Dr. Francesco Berrettini is gratefully acknowledged for the X-ray diffraction data collection for **2** and **3** at 293 K at Centro Interdipartimentale di Analisi e Determinazioni Strutturali (CIADS), Unisi.

Supporting Information Available: X-ray crystallographic data for **2** and **3** in CIF format file and tables of orthogonal atomic coordinates for selected computed molecular structures. This material is available free of charge via the Internet at http://pubs.acs.org.

IC060755S